



## The Gaia alerted fading of the FUor-type star Gaia21elv

Nagy et al. 2023

Helong Guo (郭贺龙, hlguo@ynu.edu.cn)

Yunnan University

2024-01-05

# Introduction

- Studying the accretion in young stellar objects (YSOs) is important to understand their formation. The accretion rates of YSOs are known to be highly variable, with extreme cases of eruptive YSOs, their luminosity increases up to two orders of magnitude. These events are detected as 2-5 mag brightening in optical and near-infrared (NIR) bands.
- Studies with large samples of objects indicate that young stars experience these events once every  $10^3$ – $10^4$  years (e.g. Fischer et al. 2019).
- Episodic accretion is one of the possible explanations for the observed large luminosity spread of young stellar objects (Fischer et al. 2022).
- FU Orionis objects (FUors) are well-studied examples of episodic accretion (Hartmann & Kenyon 1996). FUors are lowmass ( $< 2 M_{\odot}$ ) eruptive YSOs that exhibit large-amplitude ( $>4$  mag) outbursts at optical and infrared wavelengths and last from decades to a century.
- So far the number of confirmed FUors is limited to no more than two dozens (Audard et al. 2014). One of the important, so far unclear points is the end of the FUor outbursts, i.e. their return to quiescence.

# Introduction

- One of the best tools to discover the brightening or fading of eruptive young star candidates is the Gaia Photometric Science Alerts system, due to its large sky coverage and typically monthly cadence (Hodgkin et al. 2021).
- Several eruptive YSOs have already been discovered based on the Gaia Science Alerts. Gaia21elv (ESO H  $\alpha$  -148 or 2MASS J08410676-4052174) had a Gaia alert on 2021 October 6 due to its quick fading by 1.2 mag over 18 months.
  - RA= 08h 41m 6.75s, DEC= -40° 52' 17."44
  - It is a known young, Class II type star.
  - Its Gaia DR3 (Gaia Collaboration et al. 2022) parallax is  $1.0727 \pm 0.0397$  mas. After the zero-point correction, the Gaia DR3 parallax can be converted to a distance of  $910.9 \pm 33.7$  pc.

# OBSERVATIONS: Optical and Infrared photometry

- In 2022 June 5, 6, 8 and 9, we obtained optical photometric observations of Gaia21elv with the 60-cm Ritchey-Chrétien Rapid Eye Mount (REM) telescope operated by the Italian National Institute for Astrophysics (INAF) at La Silla (Chile) using its ROS2 instrument, an optical imager operating at four simultaneous passbands (Sloan g, r, i, z).
- Further observations between 2022 Oct 26 and 2023 Jan 4, during 12 nights. These observations, taken in Sloan g, r, i passbands.
- In 2022 June, we obtained infrared photometric observations with the REM, using the infrared imaging camera, REMIR (J, H, K).

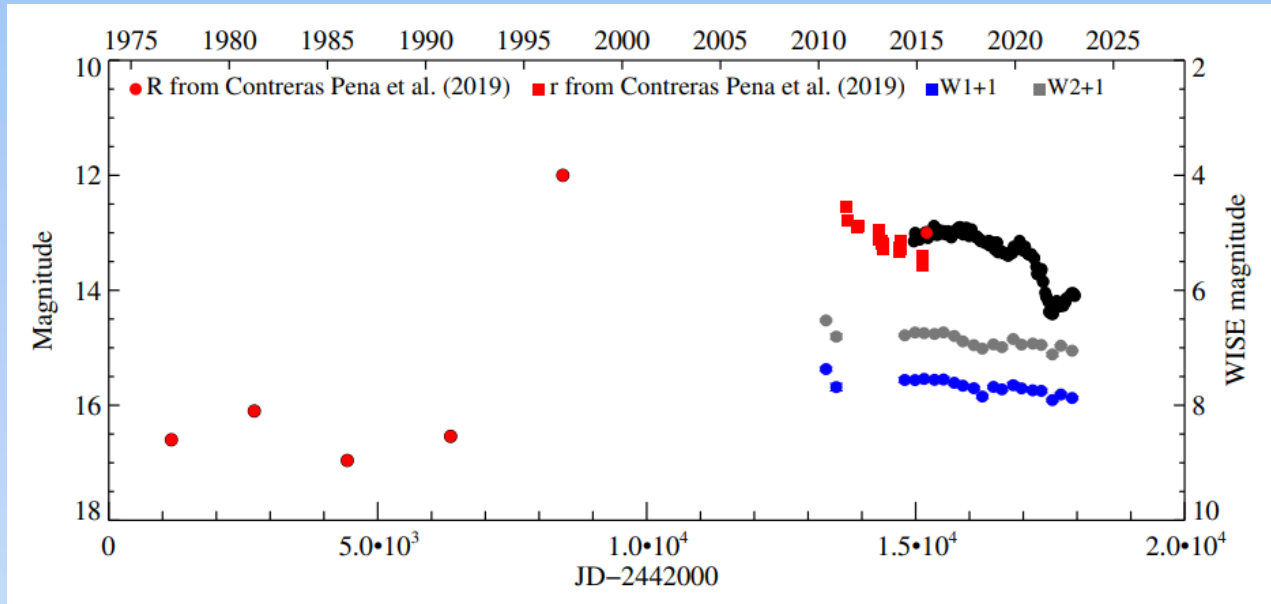
**Table A1.** REM photometry of Gaia21elv.

JD - 2 450 000	<i>g'</i>	<i>r'</i>	<i>i'</i>	<i>z'</i>	<i>J</i>	<i>H</i>	<i>K<sub>s</sub></i>
9736.50	16.91±0.10	14.81±0.03	13.51±0.03	12.63±0.05	...	...	...
9738.50	17.02±0.24	14.83±0.03	13.48±0.03	12.61±0.04	9.90±0.04	8.69±0.05	7.79±0.04
9739.47	16.84±0.08	14.89±0.02	13.57±0.02	12.67±0.04	9.91±0.06	8.71±0.06	7.79±0.09
9740.49	16.93±0.11	14.87±0.02	13.53±0.03	12.71±0.03	9.85±0.07	8.68±0.06	7.82±0.02
9878.86	...	...	...	...	9.81±0.18	...	...
9883.86	16.87±0.09	14.71±0.08	13.31±0.13	...	10.18±0.43	...	...
9889.84	16.79±0.21	14.66±0.05	13.38±0.08	...	...	...	...
9896.75	16.73±0.17	14.59±0.07	13.27±0.09	...	...	...	...
9901.86	16.92±0.15	14.67±0.09	13.35±0.15	...	...	...	...
9906.86	16.88±0.17	14.66±0.08	13.30±0.09	...	9.70±0.49	...	...
9926.72	16.79±0.21	14.61±0.12	13.28±0.09	...	...	...	...
9933.72	16.72±0.27	14.68±0.13	13.33±0.13	...	...	...	...
9938.72	16.69±0.20	14.63±0.11	13.31±0.10	...	...	...	...
9943.75	16.82±0.09	...	13.37±0.02	...	...	...	...

**Table A2.** Photometry from other telescopes obtained for Gaia21elv.

JD - 2 450 000	<i>B</i>	<i>V</i>	<i>g'</i>	<i>r'</i>	<i>i'</i>	Telescope
9867.86	18.23±0.11	15.64±0.04	...	14.20±0.14	13.04±0.08	Danish 1.54-m
9875.86	18.28±0.03	15.67±0.11	...	14.25±0.10	13.07±0.10	Danish 1.54-m
9904.69	...	15.71±0.05	...	14.43±0.06	...	PROMPT6
9908.70	17.95±0.11	15.87±0.08	...	14.42±0.06	...	UZPW 50cm
9909.68	...	15.61±0.04	...	...	13.01±0.05	PROMPT6
9911.68	...	...	16.86±0.03	14.61±0.04	13.26±0.04	UZPW 50cm
9913.82	...	...	...	14.67±0.05	13.35±0.06	UZPW 50cm
9916.84	...	...	...	14.67±0.05	13.26±0.04	UZPW 50cm
9917.84	...	...	16.91±0.04	14.53±0.07	13.28±0.05	UZPW 50cm
9920.69	...	15.65±0.06	...	14.39±0.07	13.08±0.05	PROMPT6
9925.84	...	...	16.91±0.03	14.69±0.04	13.33±0.04	UZPW 50cm
9932.65	...	...	16.94±0.03	14.70±0.04	13.31±0.04	UZPW 50cm
9934.59	...	...	16.81±0.09	14.66±0.04	13.31±0.04	UZPW 50cm
9943.58	...	...	16.87±0.04	14.66±0.05	13.28±0.05	UZPW 50cm
9946.56	...	...	16.86±0.04	14.71±0.03	13.33±0.03	UZPW 50cm
9947.57	...	...	16.91±0.03	14.69±0.03	13.28±0.03	UZPW 50cm
9949.73	...	...	16.96±0.03	14.72±0.05	13.31±0.04	UZPW 50cm
9950.84	...	...	16.93±0.04	14.70±0.04	13.31±0.03	UZPW 50cm
9952.71	...	...	16.91±0.04	14.74±0.04	13.34±0.04	UZPW 50cm
9954.61	...	15.76±0.05	...	14.44±0.07	13.16±0.06	PROMPT6
9955.86	...	...	16.95±0.03	14.71±0.03	13.34±0.05	UZPW 50cm
9959.66	...	15.70±0.06	...	14.39±0.07	13.11±0.05	PROMPT6
9962.64	...	...	16.91±0.03	14.67±0.04	13.30±0.04	UZPW 50cm
9963.73	...	...	16.89±0.02	14.65±0.03	13.28±0.04	UZPW 50cm
9964.63	...	15.65±0.06	...	14.35±0.06	13.08±0.06	PROMPT6
9966.87	...	...	16.88±0.03	...	...	UZPW 50cm
9969.62	...	15.66±0.05	...	14.36±0.07	13.09±0.05	PROMPT6

# OBSERVATIONS: Optical and Infrared photometry



Based on these data, the eruption occurred around between 1991 and 1996. The amplitude of the brightening was 4-4.5 mag from a quiescent 16.5-17 mag to around 12 mag in the R-band. A slow fading of the source is already seen after 2010 based on data points from Contreras Peña et al. (2019).

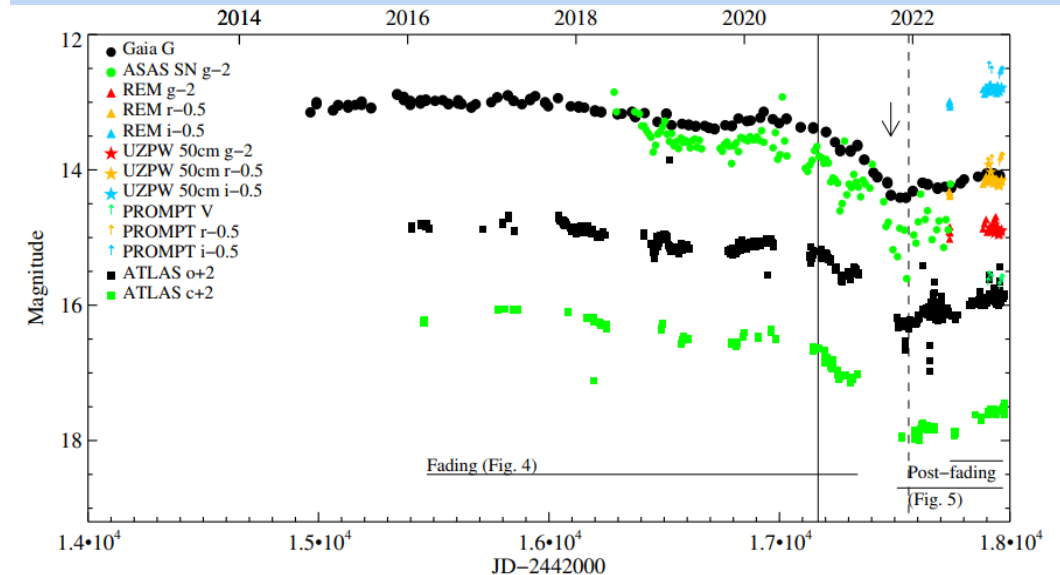


**Figure 1.** Light curve of Gaia21elv in *Gaia* G (black), *WISE* W1 (blue) and W2 (grey) bands, and in *g* band from the ASAS-SN (green). The solid vertical line shows the epoch of the Gemini/IGRINS spectrum, the dashed vertical line shows the epoch of the VLT/X-SHOOTER, and the arrow shows the epoch of the *Gaia* alert. The ranges covered by the colour-magnitude diagrams in Figures 4 and 5 during and after the fading phase, respectively, are also indicated.



# Light and colour variations

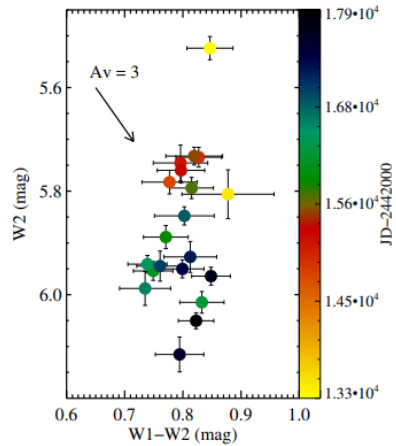


**Figure 2.** Colour-magnitude diagram based on WISE W1 and W2 data.

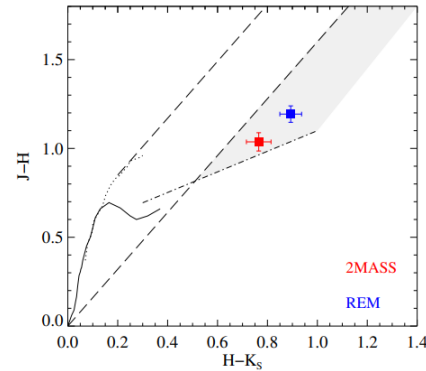


**Figure 3.**  $(J - H)$  versus  $(H - K_S)$  colour-colour diagram for the bright state (2MASS data point from 1999 February) and during the fading (REM data point from 2022 June). The solid curve shows the colours of the zero-age main-sequence, and the dotted line represents the giant branch (Bessell & Brett 1988). The long-dashed lines delimit the area occupied by the reddened normal stars (Cardelli et al. 1989). The dash-dotted line is the locus of unreddened CTTS (Meyer et al. 1997) and the grey shaded band borders the area of the reddened  $K_S$ -excess stars.

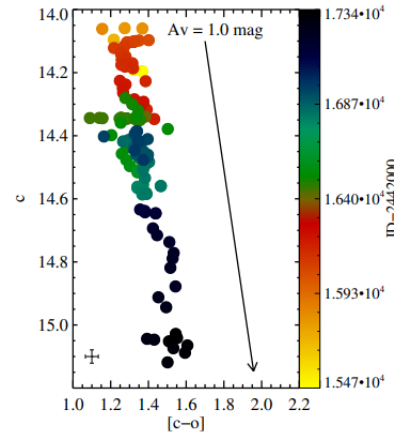


**Figure 4.** Colour-magnitude diagram based on  $o$  and  $c$  magnitudes from the ATLAS survey during the fading of Gaia21elv. The typical error bar is shown in the lower left corner.

Based on the colour variations alone, it is not possible to make a conclusion on the origin of the brightness variations of Gaia21elv. The  $o$  and  $c$  band data from the ATLAS survey as well as the  $g - r$  versus  $r$  and  $r - i$  versus  $r$  colour-magnitude diagrams suggest extinction-related brightness variations both during the fading and the brightening. Such extinction-related variations are not seen in the WISE colour-magnitude diagrams, whereas the  $J - H$  vs  $H - K$  diagram can be interpreted both as a result of extinction and accretion. Therefore, we do not make a conclusion on the origin of the brightness variations based on the colour variations,

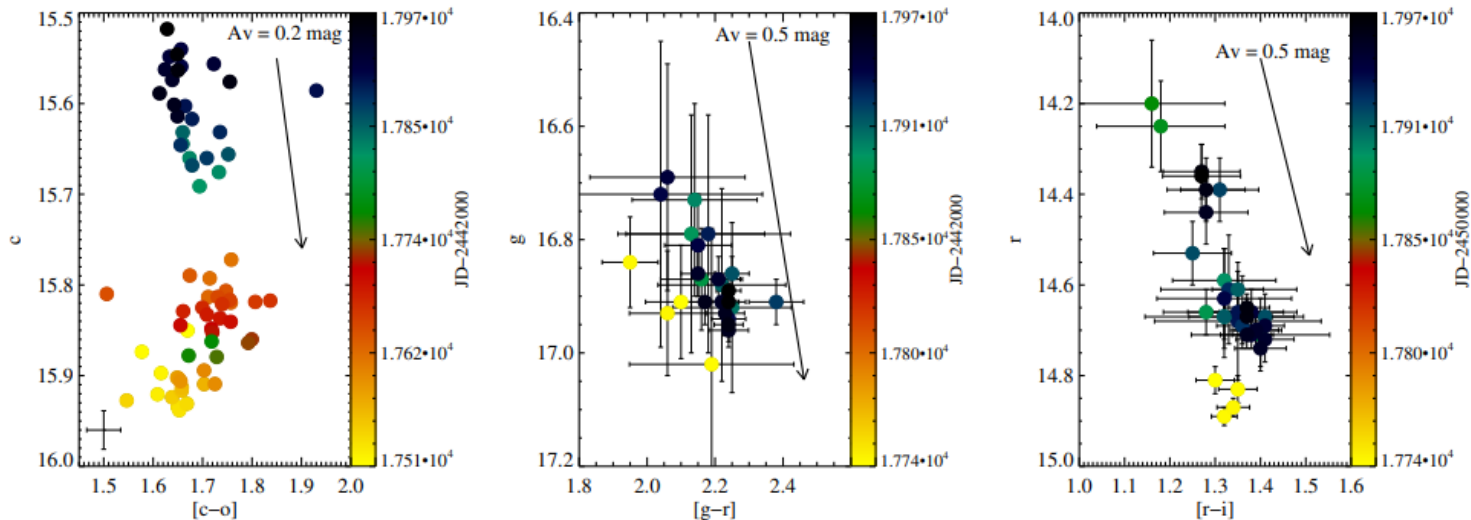


**Figure 5.** Left panel: Colour-magnitude diagram based on  $o$  and  $c$  magnitudes from the ATLAS survey after the fading of Gaia21elv. The typical error bar is shown in the lower left corner. Middle and right panels: Colour-magnitude diagrams based on follow-up photometry shown in Tables A1 and A2.

# **OBSERVATIONS: Spectroscopy**

- They obtained high-resolution ( $R \sim 45,000$ ) NIR spectra of Gaia21elv on 2020 November 14 using the Immersion GRating INfrared Spectrograph (IGRINS) of Gemini South, in the H and K bands.
- A spectrum using the X-SHOOTER instrument of the Very Large Telescope (VLT) at ESO's Paranal Observatory in Chile was taken on 2021 December 12. X-SHOOTER simultaneously covers a wavelength range from 300 nm to 2480 nm, and the spectra are divided into three arms, the ultraviolet (UVB, 300 – 550 nm), the visible (VIS, 500 – 1020 nm), and the near-infrared (NIR, 1000 – 2480 nm). The spectral resolution of  $R \sim 5400$ , 8900, and 11600 for UVB, VIS, and NIR, respectively.

# OBSERVATIONS: Spectroscopy

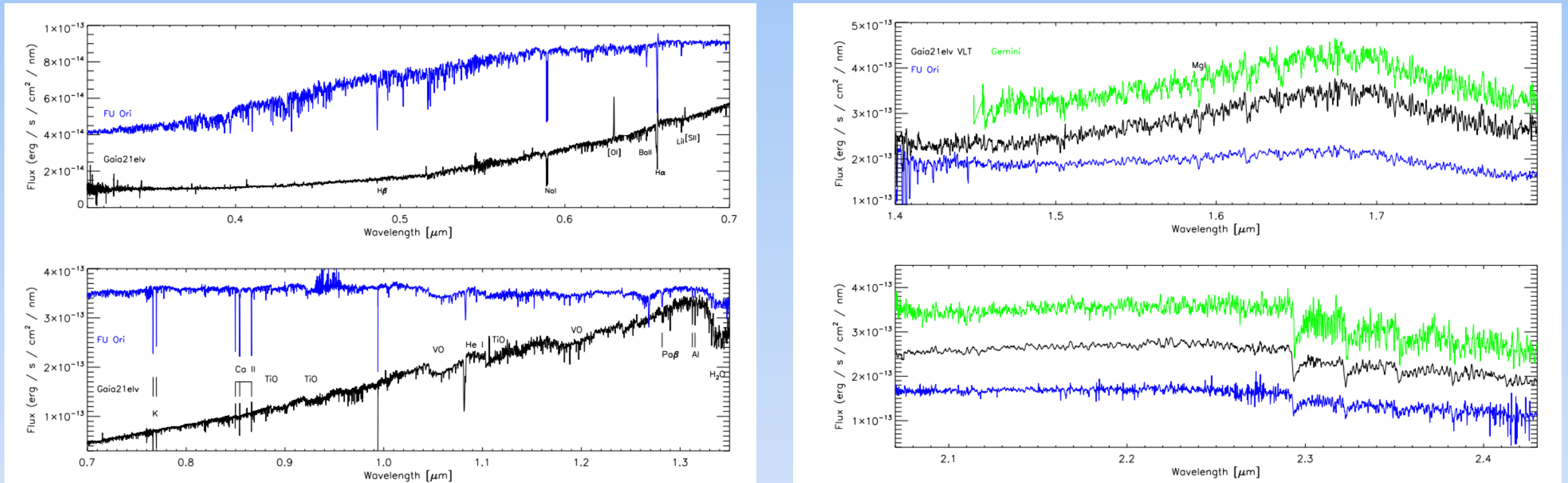


**Figure 6.** Optical and NIR spectra of Gaia21elv taken with VLT/X-SHOOTER and Gemini South/IGRINS in comparison with those of FU Ori (taken also with VLT/X-SHOOTER, ESO archival data from program 094.C-0233). Arbitrary scaling factors were applied for a better comparison of the spectra. The Gemini South/IGRINS spectrum was smoothed for a better comparison.

They used the X-SHOOTER spectrum comparing it to the spectrum of FU Ori and dereddened the spectrum of Gaia21elv with increasing  $A_v$  until it matched the scaled. They suggest  $A_v \sim 5.7$  mag for Gaia21elv in its faint state.



# OBSERVATIONS: Spectroscopy

**Table 1.** Lines detected in the X-SHOOTER spectrum of Gaia21elv. The FWHM values were derived using a Gaussian fitting, and are not provided for line profiles, which cannot be fitted by a Gaussian. For lines with multiple components, we provide the parameters of the one with the highest intensity.

Species	Lab. $\lambda$ [nm]	Obs. $\lambda$ [nm]	EW [nm]	FWHM [nm]	Note
[S II]	406.860	406.702	$-1.01 \pm 0.05$	$0.20 \pm 0.03$	emission
H $\delta$	410.171	410.038	$0.05 \pm 0.01$	$0.10 \pm 0.01$	absorption
H $\gamma$	434.047	433.850	$0.13 \pm 0.03$	$0.32 \pm 0.01$	absorption
H $\beta$	486.129	485.997	$0.13 \pm 0.01$	...	P Cygni absorption
H $\beta$	486.129	486.251	$-0.04 \pm 0.01$	$0.16 \pm 0.02$	P Cygni emission
Na D	588.995	588.898	$0.30 \pm 0.01$	$0.27 \pm 0.01$	absorption
Na D	589.592	589.508	$0.25 \pm 0.01$	$0.24 \pm 0.02$	absorption
[O I]	630.030	629.801	$-0.28 \pm 0.02$	$0.29 \pm 0.01$	emission
Ba II	649.690	649.515	$0.08 \pm 0.01$	$0.38 \pm 0.01$	absorption
H $\alpha$	656.282	656.155	$0.42 \pm 0.01$	...	P Cygni absorption
H $\alpha$	656.282	656.377	$-0.09 \pm 0.01$	$0.18 \pm 0.02$	P Cygni emission
Li I	670.776	670.785	$0.03 \pm 0.01$	$0.13 \pm 0.01$	absorption
[S II]	673.082	672.960	$-0.05 \pm 0.01$	$0.28 \pm 0.01$	emission
[Fe II]	715.517	715.364	$-0.08 \pm 0.01$	$0.24 \pm 0.01$	emission
K I	766.490	766.457	$0.15 \pm 0.01$	$0.20 \pm 0.02$	absorption
K I	769.896	769.851	$0.10 \pm 0.01$	$0.20 \pm 0.02$	absorption
Ca II	849.802	849.647	$0.05 \pm 0.01$	$0.19 \pm 0.02$	P Cygni absorption
Ca II	849.802	849.854	$-0.04 \pm 0.01$	$0.12 \pm 0.01$	P Cygni emission
Ca II	854.209	854.028	$0.10 \pm 0.01$	$0.28 \pm 0.01$	P Cygni absorption
Ca II	854.209	854.276	$-0.06 \pm 0.01$	$0.16 \pm 0.01$	P Cygni emission
Ca II	866.214	866.043	$0.09 \pm 0.01$	$0.23 \pm 0.01$	P Cygni absorption
Ca II	866.214	866.283	$-0.04 \pm 0.01$	$0.14 \pm 0.01$	P Cygni emission
Pa8	954.620	954.607	$0.04 \pm 0.01$	$0.21 \pm 0.02$	absorption
He I	1083.025	1081.46	$0.60 \pm 0.10$	$1.20 \pm 0.20$	absorption, two components
Pa $\beta$	1281.807	1281.819	...	...	absorption, two components
Al I	1312.342	1312.382	$0.06 \pm 0.01$	$0.18 \pm 0.01$	absorption
Al I	1315.075	1315.107	$0.07 \pm 0.01$	$0.22 \pm 0.01$	absorption

# Spectral Energy Distribution modeling

- we analyse the Spectral Energy Distribution (SED) of Gaia21elv at three different epochs.
  - a) The state of the maximum brightness, when the brightness of the star did not change significantly.
  - b) 2020 Oct–Nov that is very close to the epoch of the Gemini/IGRINS spectrum, and as such, it is just before the fast fading phase of the source.
  - c) The epoch of the VLT/X-SHOOTER spectrum in 2021 December, as it represents the faint state at the end of the fast fading of the source.

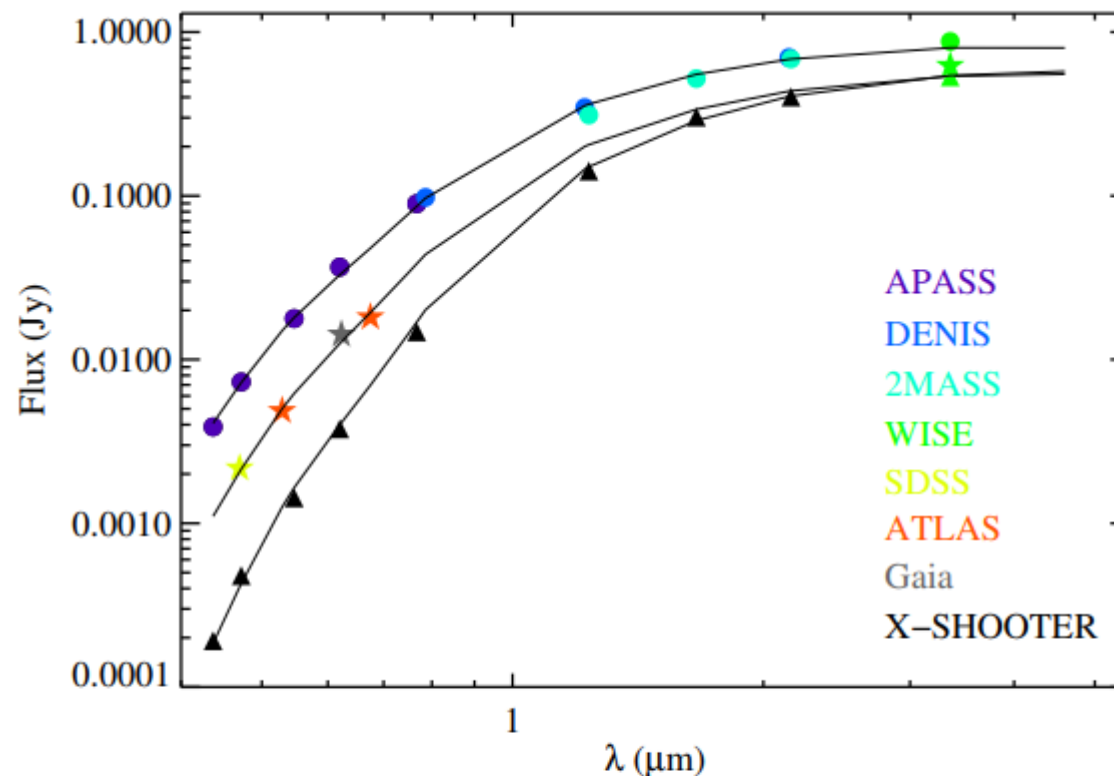


**Figure 13.** The SED of Gaia21elv at the three modelled epochs. The SED at the brightest state based on archival data is shown with circles. The SED close to the epoch of the Gemini/IGRINS spectrum is shown with asterisks. The SED at the epoch of the VLT/X-SHOOTER spectrum representing the faint state is shown with triangles. Solid curves show the results of the accretion disc models for the individual epochs.

# Spectral Energy Distribution modeling

- To estimate the properties of the accretion disc in Gaia21elv at the three epochs, they modelled the SEDs using a steady, optically thick and geometrically thin viscous accretion disc, whose mass accretion rate is constant in the radial direction. This method was successfully applied to estimate the accretion rate in several eruptive YSOs.

In this model, the temperature profile of the disc is defined based on Hartmann & Kenyon (1996) as:

$$T(r) = \left[ \frac{3GM_{\star}\dot{M}}{8\pi R_{\star}^3\sigma} \left( 1 - \sqrt{\frac{R_{\star}}{r}} \right) \right]^{1/4},$$

where  $r$  is the distance from the star,  $R_{\star}$  is the stellar radius,  $M_{\star}$  is the stellar mass,  $\dot{M}$  is the accretion rate, and  $G$ ,  $\sigma$  are the gravitational and Stefan-Boltzmann constants, respectively. The model SED was calculated by integrating black-body emission in concentric annuli between the inner disc radius and the outer disc radius. The resulting SED was then reddened by different  $A_V$  values.

They used an intermediate value of  $45^\circ$ , and fixed the inner disc radius to  $R_{\text{in}} = 2R_{\odot}$ .

Their models suggest a slight increase of the extinction toward the source from 3.6 mag to 4.4 mag between the maximum brightness and the Gemini epoch in 2020 November. The accretion luminosity of the source also dropped in parallel to the accretion rate between the first and last epoch, from  $106 L_{\odot}$  to  $68 L_{\odot}$ .

# Classification of Gaia21elv as a FUor

- To investigate, whether Gaia21elv is indeed a FUor, we used the criteria from Connelley & Reipurth (2018).

**Table 3**  
Basis of FUor Classification

Name	Eruption Observed?	CO abs.	Water abs.	VO or <sup>a</sup> TiO	Pa $\beta$ abs.	Emission Lines	Weak metals	He I abs.
Bona fide FUors								
RNO 1b	Y	Y	Y	Y	Y	N	Y	Y
V582 Aur	Y	Y	Y	Y	Y	N	Y	Y
V883 Ori	Y	Y	Y	Y	Y	N	Y	N
V2775 Ori	Y	Y	Y	Y	Y	N	Y	Y
FU Ori	Y	Y	Y	Y	Y	N	Y	Y
V900 Mon	Y	Y	Y	Y	Y	N	Y	Y
V960 Mon	Y	Y	Y	Y	Y	N	Y	Y
V1515 Cyg	Y	Y	Y	Y	Y	N	Y	Y
HBC 722	Y	Y	Y	Y	Y	N	Y	Y
V2494 Cyg	Y	Y	Y	Y	Y	Y	Y	Y
V1057 Cyg	Y	Y	Y	Y	Y	N	Y	Y
V2495 Cyg	Y	Y	Y	no data	no data	N	Y	no data
V1735 Cyg	Y	Y	Y	Y	Y	N	Y	Y
V733 Cep	Y	Y	Y	Y	Y	N	Y	N
FUor-like								
RNO 1c	N	Y	N	N	Y	N	Y	N
PP 13S	N	Y	Y	no data	no data	Y	Y	no data
L1551 IRS5	N	Y	Y	Y	N	Y	Y	N
Haro 5a/6a	N	Y	Y	no data	no data	N	Y	no data
IRAS 05450+0019	N	Y	Y	no data	N	N	Y	no data
Z CMa	N	N	N	N	N	Y	Y	Y
BBW 76	N	Y	Y	Y	Y	N	Y	Y
Parsamian 21	N	Y	Y	Y	Y	N	Y	Y
CB 230 IRS1	N	Y	Y	no data	no data	Y	Y	no data
HH 354 IRS	N	Y	Y	no data	no data	N	Y	no data
Peculiar								
V1647 Ori	Y	N	Y	Y	N	Y	Y	Y
IRAS 06297+1021W	N	N	Y	N	N	Y	Y	Y
AR 6a	N	N	N	N	Y	N	Y	Y
AR 6b	N	Y	N	no data	N	N	Y	no data
IRAS 06393+0913	N	Y	N	N	N	N	Y	no data
V346 Nor	Y	N	N	no data	no data	Y	Y	no data
V371 Ser	N	Y	Y	no data	no data	Y	Y	no data
IRAS 18270-0153W	N	N	Y	no data	no data	Y	Y	no data
IRAS 18341-0113S	N	N	Y	no data	no data	Y	Y	no data

- Bona fide FUors have well defined CO absorption features. Strong CO absorption was also observed for Gaia21elv at both of our observing epochs.

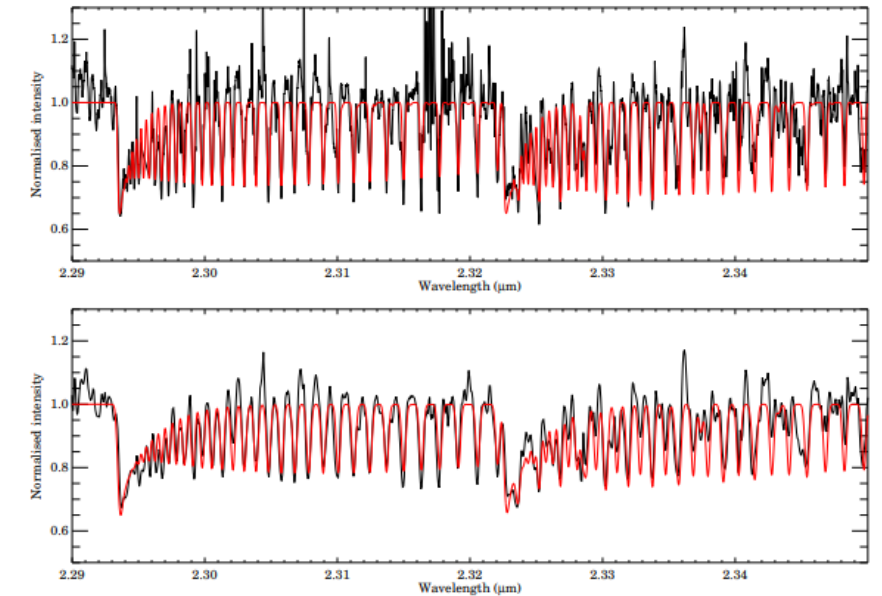


**Figure 12.** CO overtone features of Gaia21elv shown in black observed using Gemini South/IGRINS (top panel) and VLT/X-SHOOTER (bottom panel). The best fit models are overplotted in red.

# Classification of Gaia21elv as a FUor

- Water vapor bands can be identified in the NIR spectra of bona fide FUors, Gaia21elv shows these features at both epochs.
- Bona fide FUors show other molecular bands in their J-band spectra, such as those from vanadium oxide (at 1.05  $\mu\text{m}$  and 1.19  $\mu\text{m}$ ) and titanium oxide (0.88, 0.92, and 1.11  $\mu\text{m}$ ). The X-SHOOTER spectrum of Gaia21elv shows all these molecular bands as wide absorption features
- FUors show very few, if any, emission lines, and even those are typically the emission components of P Cygni profiles. Gaia21elv shows a few P Cygni profiles in  $\text{H}\alpha$ ,  $\text{H}\beta$ , and the Ca II triplet.
- FUors show weak absorption lines of Na I (2.208  $\mu\text{m}$ ) and Ca I (2.256  $\mu\text{m}$ ) (Connelley & Reipurth 2018). As shown in Fig. 11, these lines are detected in the spectra of Gaia21elv at both epochs.

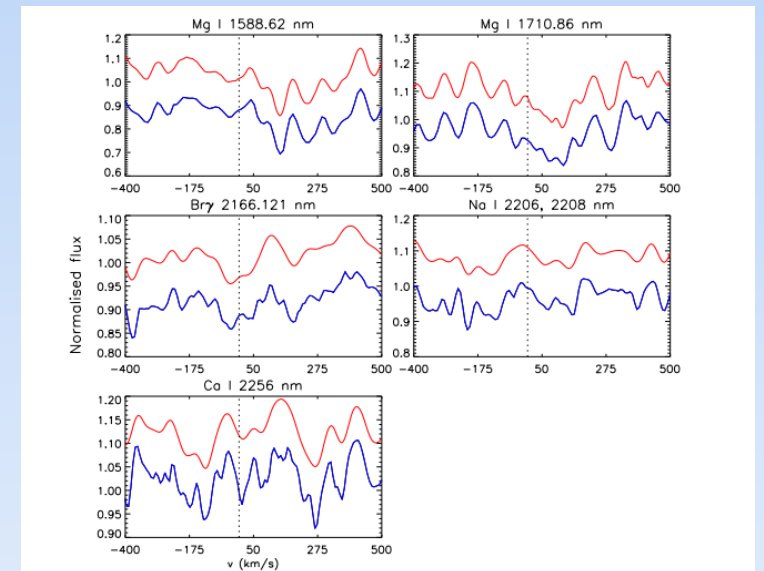
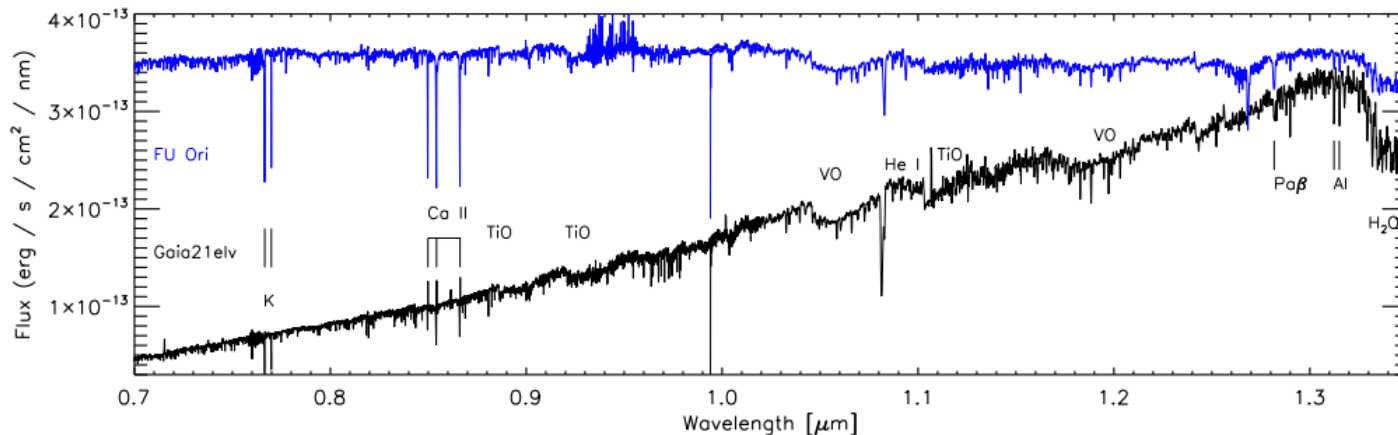


**Figure 11.** Comparison of lines detected at both epochs using Gemini South/IGRINS (red) and VLT/X-SHOOTER (blue). Arbitrary scaling factors were applied for a better comparison of the spectra.



# Classification of Gaia21elv as a FUor

- the He I line at 1.083  $\mu\text{m}$ , which is also present in the spectrum of Gaia21elv. The He I line detected toward Gaia21elv is double-peaked, where the higher intensity component is largely blueshifted, detected at a velocity of around  $-400 \text{ km s}^{-1}$ , and the lower intensity component is seen at a velocity of around  $+25 \text{ km s}^{-1}$ . Most bona fide FUors show blueshifted absorption lines, with a mean velocity of  $-350 \text{ km s}^{-1}$ .
- The hydrogen lines, especially the Pa $\alpha$ ,  $\beta$ ,  $\gamma$ , and  $\delta$  lines, are in absorption, Br $\gamma$  line is very weak, with the rest of the Brackett series not observed. For Gaia21elv the Pa $\beta$  and Pa $\delta$  lines are indeed seen in absorption, however, the other two Paschen lines are not detected.

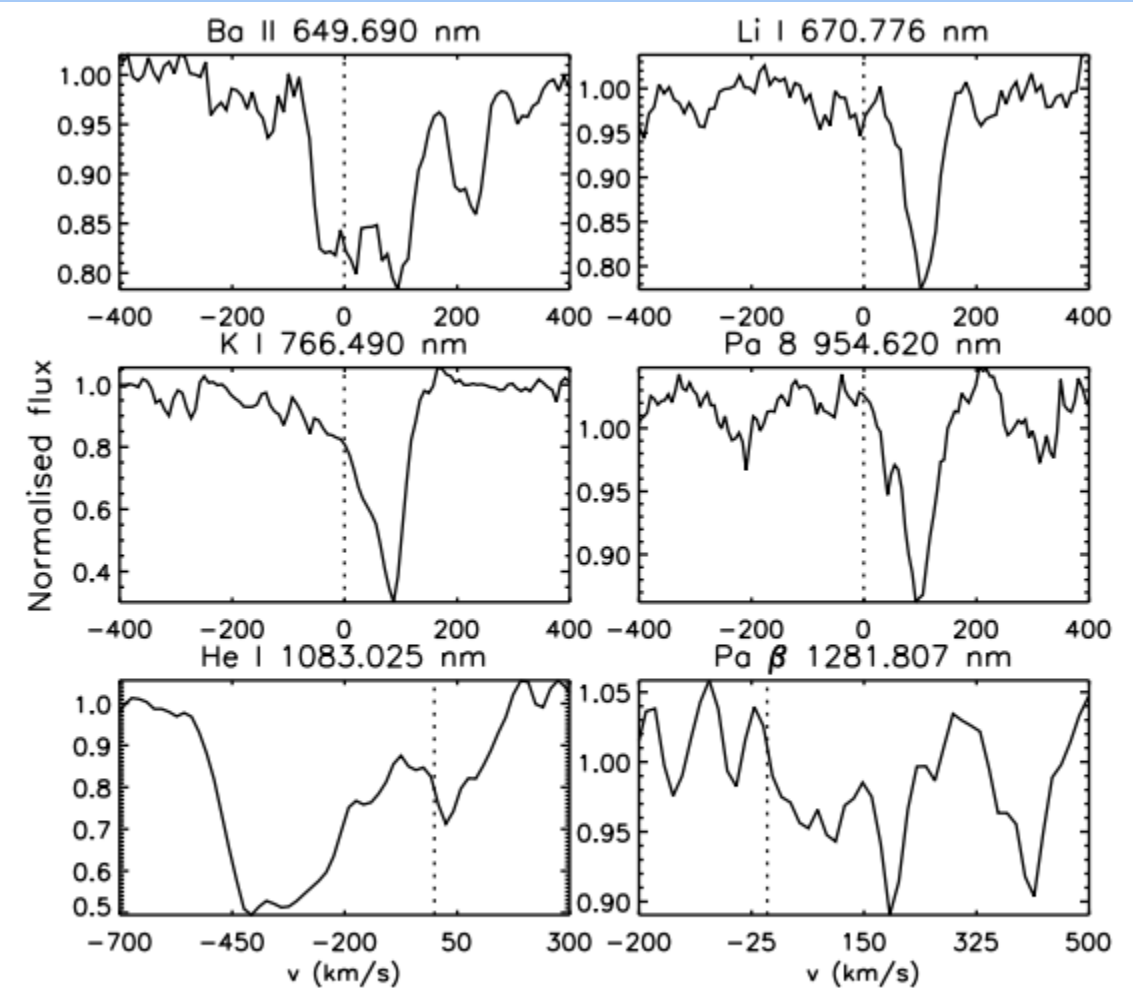


**Figure 7.** Examples of absorption lines detected toward Gaia21elv.



# Classification of Gaia21elv as a FUor

- Another characteristics of FUors is that their spectral type is wavelength-dependent. They used the VLT/X-SHOOTER spectrum, and compared it to the synthetic stellar spectra. At optical wavelengths, the best match was found with the stellar template corresponding to an effective temperature of  $5500 \pm 250$  K, while at NIR wavelengths, the best fit corresponds to an effective temperature of  $3750 \pm 250$  K which mean that the stellar type is wavelength-dependent.

Based on the above criteria from Connelley & Reipurth (2018) as well as its wavelength-dependent spectral type, we conclude that Gaia21elv can be classified as a bona field FUor. This classification is consistent with the high accretion luminosity of the source implied by our accretion disc modelling.

# SUMMARY

- We analysed the photometry and spectroscopy of a young star exhibiting a long-term outburst and a recent fading alerted by the Gaia Science Alerts system.
- Optical and NIR spectra confirm that Gaia21elv is a bona fide FUor. This is the third FUor which was found based on the Gaia alerts.
- Fitting the SEDs at the maximum brightness and its faint state using an accretion disc model suggests a decrease in the accretion rate. However, fitting the SED at an epoch close to the onset of the quick fading in late 2020-2021 indicates that this episode was mostly caused by an increase of circumstellar extinction.
- In the future, a photometric and spectroscopic monitoring of Gaia21elv is important to characterize its behavior after its fading episode.

Thanks!